Journal of Structural Geology 33 (2011) 907–917

Contents lists available at ScienceDirect

Journal of Structural Geology

journal homepage: www.elsevier.com/locate/jsg

The impact of strike-slip, transtensional and transpressional fault zones on volcanoes. Part 1: Scaled experiments

Lucie Mathieu [a,b,*,1], Benjamin van Wyk de Vries [b]

[a] Department of Geology, Museum building, Trinity College Dublin, Ireland
[b] Laboratoire de Magmas et Volcans, Blaise-Pascal University, Clermont-Ferrand, France

ARTICLE INFO

Article history:
Received 27 May 2010
Received in revised form
1 February 2011
Accepted 2 March 2011
Available online 12 March 2011

Keywords:
Strike-slip faults
Analogue models
Spreading
Volcano
Transpression
Transtension

ABSTRACT

The activity of a regional strike-slip fault can affect or channel magma migration, can deform a volcano and can destabilise the edifice flanks. The aim of this study is to determine the location, strike, dip and slip of structures that develop in a stable or gravitationally spreading volcanic cone located in the vicinity of a fault with a strike-slip component. This problem is addressed with brittle and brittle-ductile analogue models. The one hundred and twenty three models were deformed by pure strike-slip, transtensional or transpressional fault displacements. The deformation was organized around an uplift in transpressional and strike-slip experiments and around a subsiding area in transtensional experiments. Most displacements are accommodated by a curved fault called Sigmoid-I structure, which is a steep transpressional to transtensional fault. This fault projects the regional fault into the cone and delimits a summit graben that is parallel to the main horizontal stress. The systematic measurements of faults strike and slip in the experiments indicate that extension along the faults in the cone increases with the extensional component of the regional fault and the thickness of the substratum ductile layer. The distribution of the fastest horizontal movements of the analogue cone flanks, which vary depending on the regional fault characteristics and on the composition of the substratum, correspond to the distribution of instabilities in nature. Natural examples of volcanoes sited in strike-slip contexts are described and interpreted in the light of the analogue results in the second article

1. Introduction

Many volcanoes are associated with faults that facilitate the transport of magma in the crust. Active faults interact with the volcano as it grows or/and as it becomes eroded. Volcanoes are also deformed by local processes such as gravitational spreading, which has been observed worldwide (van Bemmelen, 1953; Merle and Borgia, 1996; Borgia et al., 2000). This paper examines the structure of stable and spreading conical edifices interacting with faults that have a strike-slip component of movement.

There are three types of strike-slip faults: pure strike-slip, transtensional and transpressional. They are found in every geodynamic context and are the most common fault type associated with volcanic activity. Lithospheric strike-slip faults have an average slip of 1 mm to 1 cm per year (Dusquenoy et al., 1994; Bourne et al., 1998; Groppelli and Tibaldi, 1999; Corpuz et al., 2004) and fault planes are rapidly hidden by volcanic output and fast erosion of the accumulated volcanic deposits. A volcanic edifice can be internally deformed by a strike-slip fault movement even if no structures are visible at the surface (Norini and Lagmay, 2005) or may repair itself (dyke sealing fractures, etc.) between episodes of faulting (Belousov et al., 2005).

The fault kinematics and geometries considered here have been studied by previous authors. In theory, if a cone is added on top of a flat substratum above a strike-slip fault, its load will deflect the stress field (e.g. related to regional or far-field movement). A graben parallel to the regional sigma 1 and bordered by subsidiary synthetic shear fractures, i.e. Riedel (R) shears oriented at 15° and Y shears parallel to the principal displacement zone (e.g. Sylvester, 1988), initially form at the summit of the cone (van Wyk de Vries and Merle, 1998). During the experiment, the graben extends and converts to reverse faults down the cone flanks to form curved, synthetic R shears, referred to as a Sigmoid-I structure (Lagmay et al., 2000; Norini and Lagmay, 2005). A second set of synthetic shears, i.e. P shear, develops around the summit. The P shears are named Sigmoid-II structures (Lagmay et al., 2000) and border a fast moving summit area (Andrade, 2009; e.g. Fig. 1-b). In addition to these

* Corresponding author. Department of Geology, Museum building, Trinity College Dublin, Ireland.
E-mail address: mathiel@tcd.ie (L. Mathieu).
[1] Permanent address: 12 allée du chevalier de Louville, 45800 Saint Jean de Braye, France. Tel.: +33 238 700277.

0191-8141/$ – see front matter © 2011 Elsevier Ltd. All rights reserved.
doi:10.1016/j.jsg.2011.03.002

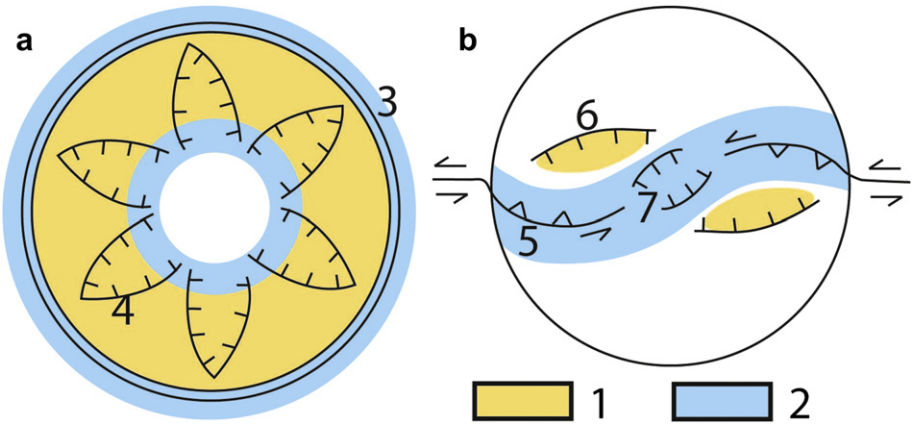

Fig. 1. Sketch of the main structures that form in an experimental cone located (a) above a ductile substratum (after Merle and Borgia, 1996) or (b) above a strike-slip fault (after Lagmay et al., 2000). The slowest and fastest horizontal movements are drawn after Delcamp et al. (2008) (a) and Andrade (2009) (b); (1) fastest and (2) slowest horizontal movements, (3) basal fold or reverse fault, (4) radial half-grabens or flower structures, (5) Sigmoid-I, (6) Sigmoid-II, (7) summit graben.

structures, folds are observed in the substratum, at the tip of Sigmoid-I faults (van Wyk de Vries and Merle, 1998). The aim of the previously published analogue modelling work was to explore the basic principles of strike-slip faults and volcanoes interaction (van Wyk de Vries and Merle, 1998) and to establish a link between regional strike-slip faults and the frequent sector collapses that affect cone-shaped volcanic edifices (Lagmay et al., 2000; Norini et al., 2008; Wooller et al., 2009). The aim of this study is to fully document the orientation, kinematics and slip rate of the Sigmoid structures. We make detailed observations on fault and fracture patterns by using a fine ignimbrite-derived powder for the modelling and we couple structural maps of the models with displacement maps to further explore the deformation of the volcanic cone's flanks.

Cones interacting with transtensional and transpressional fault planes located 10° and 20° from their strike-slip component of movement have been modelled by Andrade (2009). In these models, Sigmoid-II is a wide fracture zone in the mid-upper cone, which becomes part of the summit graben (transtension) and connects with Sigmoid-I at the cone base (transtension) or at the summit (transpression). The summit graben subsides the least and is the narrowest in transpressional experiments. The artificial North of Andrade's (2009) models is normal to the strike-slip component of movement, which strikes 090°. In these models, the summit graben strikes 040°–050° (sinistral transtension) and 060°–070° (sinistral transpression) and corresponds to the maximum rotation. The models presented in this paper build up on Andrade's (2009) pioneer study. We increase the extensional and compressional components of our faults and we quantify precisely the kinematics of each observed structure in order to better characterise the mechanisms of cone flank rotation.

Other studies have tested the volcano spreading mechanisms, which is a relevant process that controls the slow-rate and long-term structural and magmatic evolution of a volcano (e.g. Borgia, 1994). Spreading occurs at volcanoes which are underlain by a substratum containing a low-viscosity layer. The excess load (volcano) drives outward spreading movements, which form concentric thrusts and folds or sub-radial strike-slip faults in the substratum around the edifice (Merle and Borgia, 1996). The volcano is in turn affected by radial stretching and displays radial intersecting grabens, named flower grabens, and a fractured summit area (Fig. 1-b). The basic interaction between strike-slip faults and volcano spreading was described by van Wyk de Vries and Merle (1998). These authors predicted, that through theoretical considerations, the geometry of spreading-related structures (flower grabens) was expected to be disturbed by the strike-slip faulting. From this basic work, we use the analogue models to quantify the interaction between the spreading structures and a range of transtensional to transpressional fault movements, and we describe the resulting deformation fields.

The study is presented in a two-part paper. This article (part 1) employs analogue experiments to investigate the geometry of structures related to strike-slip movements in volcanic cones. Scaled analogue models are particularly useful, as the key parameters that influence the structural development can be determined by varying the experimental boundary conditions, which is not feasible in field studies. Both stable cones (Brittle substratum experiments) and spreading cones (Ductile substratum experiements) are modeled in this paper. The models were carried out in the Laboratoire de Magmas et Volcans, Blaise-Pascal University, Clermont-Ferrand, France. Part 2 investigates natural examples and compares them with the analogue models (Mathieu et al., 2011).

2. Experimental device, material and scaling

2.1. Material used

The substratum and the volcanic cone were modeled by a granular material. A first set of 112 experiments was carried out with fine-grained ignimbrite powder and 11 experiments were made with sand. Ignimbrite powder allows the development of a large number of faults and has enabled the quantification of fault kinematics, including slip and strike. This is because the ignimbrite powder preserves very clearly the fine-scale features, giving a much finer detail than sand (cf. Fig. 2). The powder is composed of sieved Grande Nappe Ignimbrite, from the Mont Dore volcano, France, consisting of angular glass and quartz grains less than 250 μm in diameter. The ignimbrite powder has an angle of internal friction of 38° and is more cohesive (100–230 Pa; Table 1) than sand (0–10 Pa) because the smallest grains (about 1 μm in size) block the pore spaces in the powder, and the grains are more angular. The sieved ignimbrite is similar to other analogue model granular materials as it fails in tension when unconfined and, when confined, fails with shear band formation. Sand is used in 11 experiments because it is easy to dye and is permeable, so, in contrast to ignimbrite, can be wet and sliced at the end of experiments to provide cross sections. The silicone Polydimethylsiloxan (PDMS), a linear viscous polymer (e.g. ten Grotenhuis et al., 2002) is used as a ductile substratum horizon in 51 experiments (cf. Table 2).

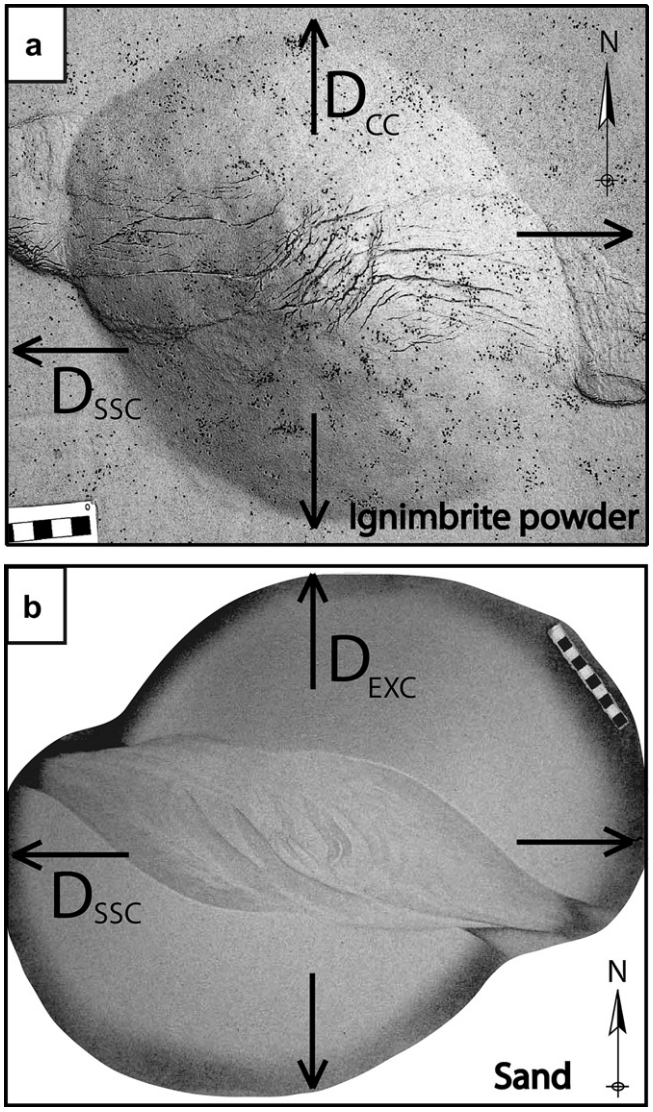

Fig. 2. Pictures of ignimbrite powder (a) and sand (b) analogue cones of Brittle substratum experiments: a) Transpression experiment ($\alpha = 20°$); b) Transtension experiment ($\alpha = 20°$).

2.2. Scaling

The scaling used here is similar to that employed in analogue experimental studies by Merle and Vendeville (1995), Donnadieu and Merle (1998) and Holohan et al. (2008). In our models 1 cm represents 1 km in nature giving a geometric scaling (e.g. ratio of model over nature length) of $H^* = 10^{-5}$ (Table 1). The stress ratio, calculated from density, gravity, and length scales is $\sigma^* = \rho^*.g^*.H^* = 5.10^{-6}$, meaning that models are about 10^6 times weaker than natural examples. To scale viscosity and time we use the viscosity ratio (μ^*) and the stress ratio (σ^*) in: $t^* = \mu^*/\sigma^*$. The time ratio (t^*) is 10^{-10} and the viscosity ratio (μ^*) is 5.10^{-16}. The natural viscosity of unconsolidated claystone or other weak sediments is about 10^{16}–10^{19} Pa s (Merle and Borgia, 1996; Delcamp et al., 2008). For technical reasons, we choose an upper value of 2.10^{19} Pa s for the natural viscosity of the weak substrata. The fault velocity in the experiment is 4 cm h^{-1}. According to the geometric scaling (1 cm represents 1 km) and the time scaling (1 h represents about $1.1{\cdot}10^6$ years), the experimental fault represents a natural fault with a slip velocity of 4 km per $1.1.10^6$ yr, that is 0.35 cm yr^{-1}, which is within the range of the estimated velocity of strike-slip faults (e.g. Dusquenoy et al., 1994; Groppelli and Tibaldi, 1999; Corpuz et al., 2004). This velocity was chosen for technical reasons.

Sand experiments are scaled with the same geometric scaling (H^*) and stress ratio (σ^*). These experiments are entirely brittle (cf. Table 2) so time is not scaled.

2.3. Experimental device

The models comprise a flat substratum, overlain by a cone. As the experiments aim to constrain the influence of regional faults and the presence of a ductile layer in the substratum, they do not consider dipping substratum, hypovolcanic complexes, hydrothermal systems or earthquakes. The angle α corresponds to the azimuth between the experimental fault plane (e.g. regional fault) and the strike-slip component of movement (e.g. D_{SSC}, Figs. 2 and 3).

In order to simplify the presentation of the experimental results, two conventions are introduced. The fault located in the substratum, beneath the analogue volcanic cone, is referred to as the regional fault. Also, a north is artificially added to the experiments. This north is normal to the regional strike-slip fault in strike-slip experiments and is parallel to the extension and compression directions in transtensional and transpressional experiments, respectively. In the following text, each strike value is given in degrees counted clockwise from the artificial north. For convenience, D_{SSC} strikes 090° and the extensional (D_{EXC}) and compressional (D_{CC}) components of movement strike 000°. The regional fault plane strikes 090° ($\alpha = 0°$;

Table 1
Parameters used to scale the ignimbrite powder experiments.

Variable	Definition	Model	Nature	Unit	Ratio*
Hc	Height of the cone	$4.4–9.10^{-2}$	$4.4–9.10^3$	m	10^{-5}
$Ø_C$	Cone diameter	0.18–0.33	$1.8–3.3.10^4$	m	10^{-5}
Hh	Total thickness of substratum	0.02	2000	m	10^{-5}
Hb	Thickness of substratum located above the ductile layer	$0–7.5.10^{-3}$	0–750	m	10^{-5}
Hs	Ductile layer thickness	$0–7.5.10^{-3}$	0–750	m	10^{-5}
β	Cone slope	10°–30°	10°–30°	/	1
Φ_I	Angle of internal friction	35–40	30–40	/	~1
τ_I	Cohesion of substratum	100	2.10^7	Pa	5.10^{-6}
g	Gravitational acceleration	9.81	9.81	m s^{-2}	1
μ_S	Ductile layer viscosity	10^4	2.10^{19}	Pa s	5.10^{-16}
t	Time	65 min	$1.2.10^6$ yr	/	10^{-10}
α	Angle between the regional fault plane and the strike-slip component of movement	0°; 20°;40°	0°; 20°;40°	/	1
D_{EXC}	Extensional component of movement of the regional fault plane	$1.8–3.5.10^{-2}$	$1.8–3.5.10^3$	m	10^{-5}
D_{CC}**	Compressional component of movement of the regional fault plane	$-1.8–3.5.10^{-2}$	$-1.8–3.5.10^3$	m	10^{-5}
D_{SSC}	Strike-slip component of movement of the regional fault plane	4.10^{-2}	4.10^3	m	10^{-5}

*Ratio of model 616 over nature variables; **DCC is negative by convention.

Table 2
Experimental setups.

	Brittle substratum	Offset (Brittle substratum)	Ductile substratum	Offset (Ductile substratum)
Ignimbrite powder (112*) **Sand**** **(11)**	42/**11**	19	36	15
Strike-slip faults (14)	5	2	"fast"*** (3)	"fast" (1)
			"slow" (2)	"slow" (1)
Transpressional (49/**5**)	17/**5**	10	"fast" (8)	"fast" (3)
			"slow" (8)	"slow" (3)
Transtensional (49/**6**)	20/**6**	7	"fast" (8)	"fast" (4)
			"slow" (7)	"slow" (3)

*amount of experiments; **The amount of sand experiments is given in bold character when it is not null; ***"fast spreading" and "slow spreading" experiments.

D_{SSC} = 100%), 110° (α = 20°; D_{SSC} = 69%) and 140° (α = 40°; D_{SSC} = 53%). The movement is left-lateral in the bulk of experiments.

The substratum has a constant thickness (Hh = 2 cm) and the models are deformed at a constant velocity (D_{SSC} = 4 cm h^{-1}) for 65 min. The intensity and velocity of the spread depend on the cone height (Hc; cf. Table 1) and slope (β, load) and on the thickness and depth of the ductile layer (Hs) and on the thickness of the substratum above the ductile layer (Hb, Merle and Borgia, 1996). From our experiments, we analyzed the influence of these individual parameters on the magnitude and velocity of the spreading, with the aim to distinguish spreading-related structures from regional fault-related structures. The experiments made with a ductile layer are divided in two subsets: "fast spreading" experiments with a ratio Hb/Hs = 0 and "slow spreading" experiments with Hb/Hs>0 (e.g. Merle and Borgia, 1996 for a discussion on the Hb/Hs ratio).

In summary, the Brittle substratum experiments are named Strike-slip, Transtensional and Transpressional experiments. The Transtensional and Transpressional experiments comprise 2 subsetups for which the value of the angle α varies. When these setups were made with sand, they were sliced at the end of the experiment. For Ignimbrite powder experiments only, a ductile substratum was added to half of the experiments, and the new setups are sub-divided between the "fast spreading" and "slow spreading" experiments. Then, an additional parameter was added to these experimental setups: a distance was introduced between the cone's summit and the regional fault plane. This last setup is called an Offset experiment (cf. Table 2).

The 112 ignimbrite powder and 11 sand models are made in a large box (e.g. $Ø_C$ = 25–35% of the box length) to avoid border effects (e.g. Fig. 3). Two plastic plates cut along the 090° (α = 0°), 110° (α = 20°) or 140° (α = 40°) directions are placed at the bottom of the box. Each plate is attached to a screw-jack connected to a motor, which is itself controlled by a computer. This system allows a continuous and constant displacement of plates parallel to D_{SSC}.

The cone and its substratum are placed in the box. A thin layer of ignimbrite powder is then sieved over the experimental device to smooth the surface and black markers (grains of hematite) are dropped over it. The surface deformation is recorded every 2 min by vertical overhead photography.

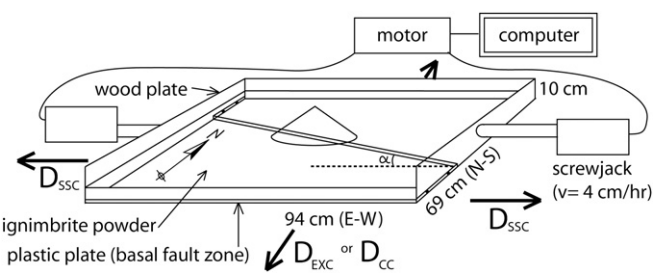

Fig. 3. Experimental setup.

The cones of sand experiments are made of several layers of dyed sand, which are used as reference horizons to quantify fault movements. At the end of the experiment the model is sprinkled with additional sand, wet with soapy water and sliced in 10–15 cross-sections. Three sets of brittle substratum experiments (α = 0°, 20° and 40°) are carried and cut normal to the fault plane, parallel to D_{EXC}-D_{CC} or parallel to D_{SSC}.

2.4. Analysis and dimensionless numbers

The cross-sections made from sand experiments enable measurement of the dip and to the amount of dip-slip of faults. The pictures of experiment surfaces are used to determine the geometry and kinematics of faults and to measure their strike. The horizontal displacements (fault slip) are quantified using a Matlab code (Point Catcher), developed by M. James (Delcamp et al., 2008). The code detects the black markers at the surface of the experiment and follows their displacement from one picture to another. The code produces several vector maps of the displacements which have occurred between successive shots. The amplitude of movement is represented by a contour map using the software "Surfer". The quantitative data obtained during the experiments are analysed with dimensionless numbers (Table 3).

3. Results

The morphology and strike of the structures observed in each experimental setup (Strike-slip, Transtensional, Transpressional and Offset experiments) are described and illustrated by Figs. 4–8. Refer to Mathieu (2010) for a more detailed description of the experiments.

In pure strike-slip experiments, the Sigmoid-I sinistral transpressional fault strikes 070° and curves at the summit of the cone where it is a 050° striking transtensional fault zone (Fig. 4-a). Sigmoid-II are 030°–040° – 070° striking dextral transtensional faults that develop in the upper cone and border an area of fast horizontal movements (Fig. 4-c). The addition of a ductile layer forms shallow 090° and 030° striking grabens in the cone (Fig. 4-b) and the NW and SE cone flanks have the fastest horizontal movements (Fig. 4-d).

In transpressional experiments, the Sigmoid-I sinistral transpressional faults strike 100° and curve at the summit where they from a 020°–040° (α = 20°) or 070° (α = 40°) striking fault zone (Fig. 5-a, b). The Sigmoid-II sinistral transtensional faults form throughout the experiments and strike 090°–120° (Fig. 5-a, b). The area of slow horizontal movements that corresponds to the Sigmoid-I fault zone rotates anti-clockwise throughout the experiment (Fig. 5-c, d). The cross-sections indicate that the movements are organised around an uplift and that the Sigmoid-II are superficial structures formed at the back of the uplift (Fig. 6-a). The addition of a ductile substratum forms 090°–100° and 040° (α = 20°) or 110°–120° and 060°–070° (α = 40°) striking grabens in

Table 3
Dimensionless numbers.

II	Number	Description
II_1	width fault zone/$Ø_C$	width of the fault zone normalised to the cone diameter (dimensionless fault width)
II_2	(D_{EXC} or D_{CC}/D_{SSC}).100 (D_{SSC}/D_{EXC} or D_{CC}).100	Percentage of extension or compression versus the strike-slip component of movement; regional fault (dimensionless regional obliquity)
II_3	($D_{EXC\text{-}C}$ or $V_{CC\text{-}C}$/$D_{SSC\text{-}C}$).100 ($D_{SSC\text{-}C}$/$D_{EXC\text{-}C}$ or $D_{CC\text{-}C}$).100	Idem for the faults developing in the cone (dimensionless edifice obliquity)
II_4	$\lvert D_{EXC\text{-}C}$ or $D_{CC\text{-}C}/D_{EXC}$ or $D_{CC}\rvert$	Extensional or compressional components of movement of cone faults normalised to the regional fault components of movement (dimensionless cone to base normal ratio)
II_5	$D_{SSC\text{-}C}/D_{SSC}$	Idem for the strike-slip component of movement (dimensionless cone to base strike-slip ratio)
II_6	offset/$Ø_C$	Distance between the regional fault zone and the cone summit normalised to the cone diameter

the cone (Fig. 5-f) and the NNW and SSE cone flanks have the fastest horizontal movements (Fig. 5-e).

In transtensional experiments, the Sigmoid-I sinistral transtensional fault strikes 080°–090° ($\alpha = 20°$) or 070° ($\alpha = 40°$) and curves at the summit where it is a 040° ($\alpha = 20°$) or 020° ($\alpha = 40°$) striking shallow graben (Fig. 7-a). The Sigmoid-II dextral transtensional faults strike 060° ($\alpha = 20°$) or 040° ($\alpha = 40°$). The deep graben bordered by Sigmoid-I and II structures (e.g. Fig. 6-b) is parallel to the regional fault plane and contains several 170°–010° striking half-grabens. The fastest horizontal movements are located on each side of the shallow summit graben (Fig. 7-c). The addition of a ductile layer forms a shallower graben parallel to the regional fault plane. This graben is bordered by broad Sigmoid-I and II fault zones and shallow 020° ($\alpha = 20°$) or 010° ($\alpha = 40°$) striking summit grabens (Fig. 7-b). The NE and SW cone flanks have the fastest horizontal movements (Fig. 7-d).

In Offset experiments (e.g. $II_6 > 0$), the largest half-cone is named part A (south) and the smallest is named part B (north; e.g. Fig. 8). On the part A of the cone, the Sigmoid-I is poorly developed and Sigmoid-II has a large extensional component of movement. On the opposite side (part B), Sigmoid-II is reduced to absent and Sigmoid-I is a broad fault zone which extends over a large area from the cone flank to the cone base.

4. Discussion

4.1. Fault geometry

One of the most important results concerns the location, strike and kinematics of faults that have developed in the cones. The synthetic Sigmoid-I fault, which is observed in strike-slip experiments, is transpressional along most of its length and transtensional at the cone summit (Fig. 8), where it borders the zone of summit subsidence. The Sigmoid-I fault defines an area of slow horizontal movements (cf. displacement maps) for two reasons: 1) it accommodates a large amount of vertical movement and 2) it is a major strike-slip fault along which movements are inversed and are equal to zero along the fault plane.

The profiles obtained with cross-cut transpressional experiments indicate that most movements are organised around an uplift, which is parallel to the regional fault zone in the early stage of the experiment. The uplifted area then rotates anti-clockwise. Once the deformation is sufficient, the synthetic transpressional Sigmoid-I faults develop at the front of the extruded material. Note that these faults are steep (dip = 50°) because they accommodate strike-slip movements in addition to reverse movements. Sigmoid-II synthetic transtensional faults are parallel to Sigmoid-I and develop at the back of the extruded matter to accommodate the extension linked to the material movement. These faults have a limited slip, are a by-product of the uplift development and do not border any summit extension. The summit transtensional faults, or central part of Sigmoid-I, do not rotate and accommodate summit subsidence. The

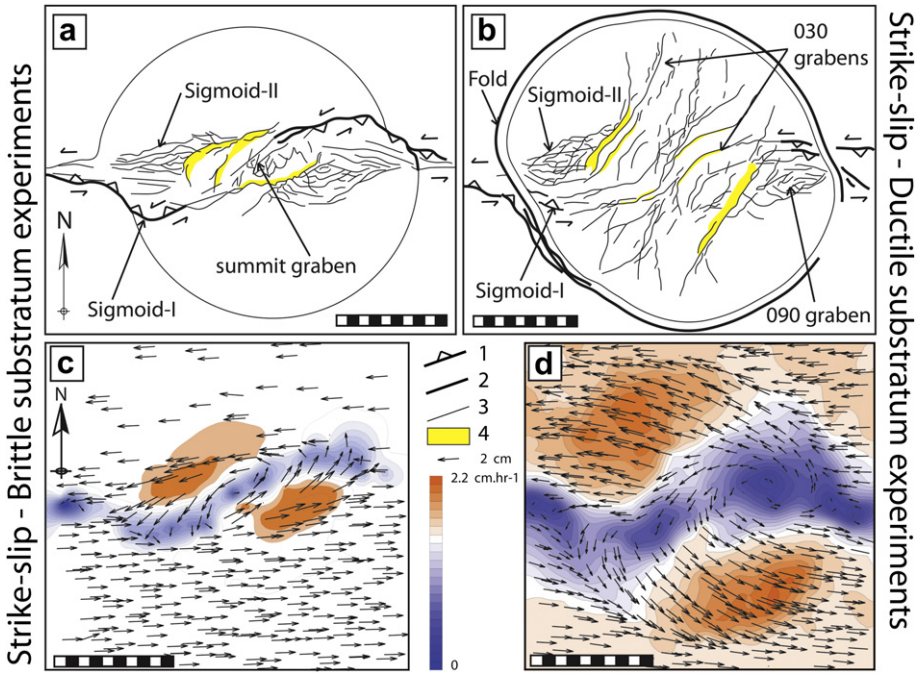

Fig. 4. a) Sketch of brittle substratum and (b) ductile substratum strike-slip experiments; c-d) Maps of the amplitude and direction of horizontal movements of (c) brittle substratum experiment for D_{SSC} = 15–18 mm and (d) of ductile substratum experiment for D_{SSC} = 7–11 mm; (1) transpressional and (3) transtensional faults, (2) folds, (4) fault plane.

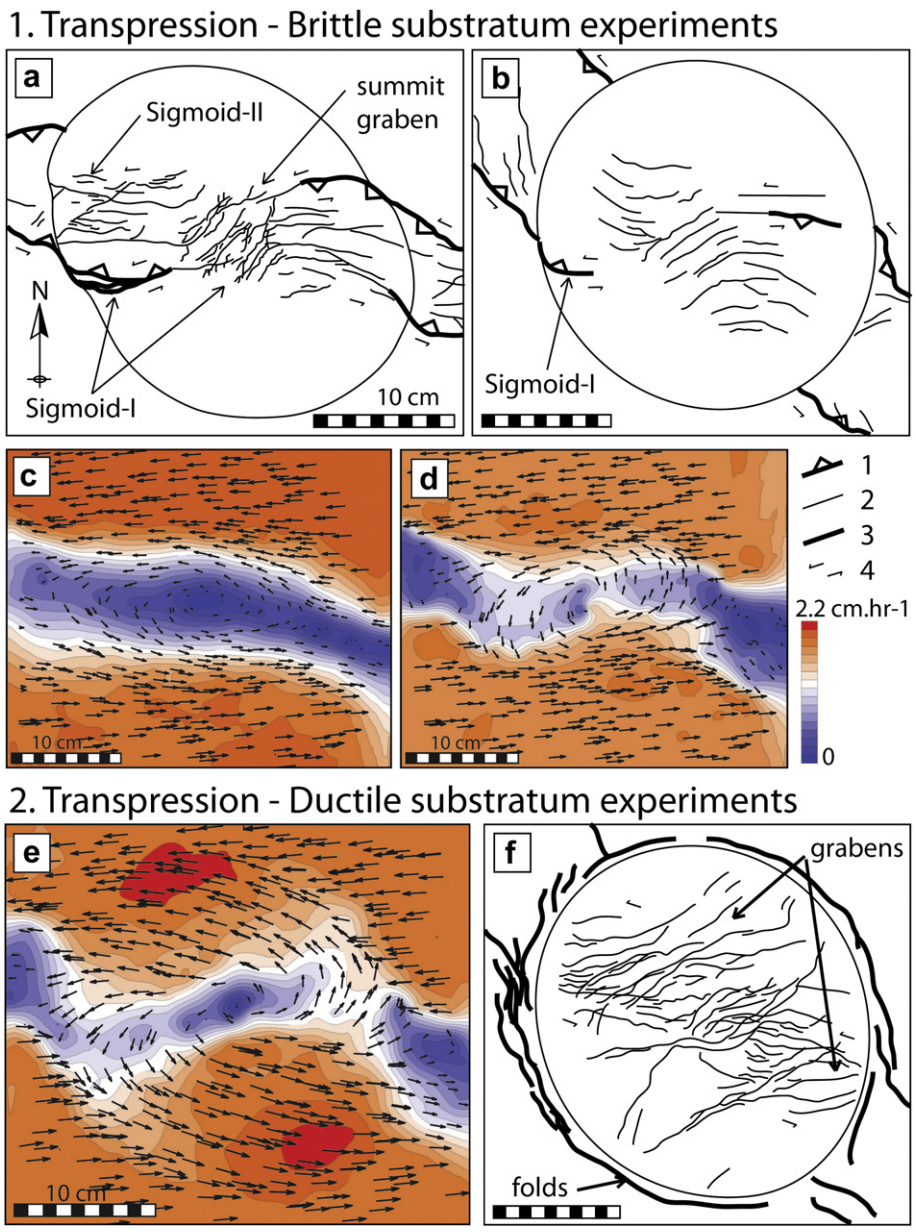

Fig. 5. a-b) Sketch of transpressional experiments with a brittle substratum and with (a) $\alpha = 20°$ and (b) $\alpha = 40°$ and experiments with a (f) ductile substratum and $\alpha = 40°$; c-d-e) Maps of the amplitude and direction of horizontal movements of (c–d) brittle substratum experiment for (c) D_{SSC} = 7–11 mm and (d) D_{SSC} = 26–30 mm and (e) of ductile substratum experiment for D_{SSC} = 18–22 mm; (1) transpressional and (2) transtensional faults, (3) folds and reverse faults, (4) strike-slip movements.

strike-slip experiments are similar to transpressional experiments and the movements may also be organised around an uplifted area. The main difference is that, in strike-slip experiments, Sigmoid-II faults are better developed transtensional faults, which border a subsiding area around the Sigmoid-I summit graben.

In transtensional experiments, Sigmoid-I faults (steep dip of 70° and limited dip-slip of 0.2–0.6 cm) and Sigmoid-II faults (shallow dip of 55° and large dip-slip of 2 cm) border a deep graben, which is parallel to the regional fault zone (Fig. 8). The graben or fault zone is narrow at the cone base and wider at the summit. It develops under the influence of the N–S directed extensional field (e.g. D_{EXC}). The numerous 000° striking half-grabens located inside the fault zone develop in an E-W directed extensional stress field.

A rotation of the early formed summit fractures is occasionally observed but the main active cone faults did not rotate. Note that this absence of rotation is in contradiction with observations from Andrade (2009). The displacement maps indicate that the highly fractured summit material is rotated anti-clockwise in the cone, for a sinistral regional fault. This rotation affects also the uplifted material of transpressional, and possibly of strike-slip, experiments. Sigmoid-I and II faults did not rotate but accommodate the rotation of the material between them.

The experiments have in common a well developed Sigmoid-I fault, the central part of which delimits a summit graben. Note that this graben has been observed by van Wyk de Vries and Merle (1998), Lagmay et al. (2000), Norini and Lagmay (2005), Andrade (2009).Sigmoid-II is either absent (transpressional experiments), restricted to the cone upper flanks (strike-slip experiments) or well developed (transtensional experiments). Sigmoid-II accommodates extension and connects with the Sigmoid-I fault at the cone base (transtensional experiments) or at mid-slope (strike-slip experiments), as already reported by Andrade (2009). The material either

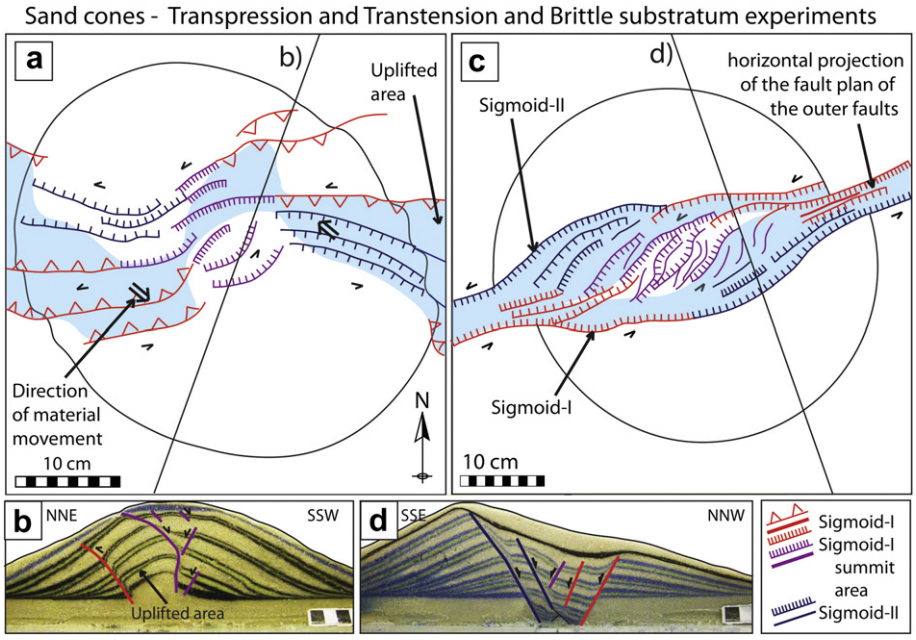

Fig. 6. Sketch and pictures of sand experiments; Structural map and profile of (a–b) transpressional and (c–d) transtensional experiments with a brittle substratum.

subsides (transtensional experiments) or is uplifted in the cone above the regional fault zone (transpressional and strike-slip experiments). Rapid summit extension is only observed in strike-slip and transtensional experiments.

4.2. Fault orientation

The strike of Sigmoid-I, II and summit faults in the bulk of experiments is determined by the regional fault geometry (kinematics and angle α of basal plates). Sigmoid-I and II faults develop $10°–20°$ from the regional fault zone. They may develop in P shears (Sigmoid-II) and R shears (Sigmoid-I) associated with this fault zone, as reported by Lagmay et al. (2000), but they do not systematically have the same kinematics as the P and R shears defined by Sylvester (1988). Indeed, P and R shears are synthetic faults (Sylvester, 1988) while Sigmoid-II is antithetic in strike-slip and transtensional experiments. Sigmoid-I and II faults thus, do not correspond to P and R shears: they are slightly oblique ($10°–20°$) to the regional fault zone because they adapt to the geometry of the cone in which they develop.

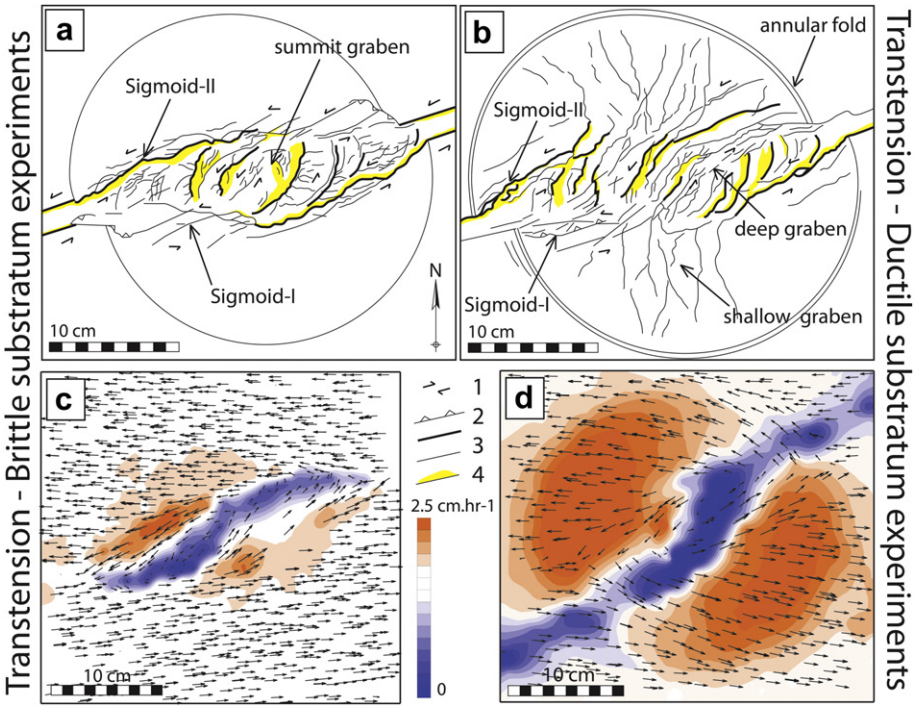

Fig. 7. a) Sketch of brittle substratum and (b) ductile substratum transtensional experiments ($\alpha = 20°$); c-d) Maps of the amplitude and direction of horizontal movements of (c) brittle substratum experiment for $D_{SSC} = 28–32$ mm ($\alpha = 20°$) and (d) of ductile substratum experiment for $D_{SSC} = 8–10$ mm ($\alpha = 40°$); (1) strike-slip movements, (2) transpressional faults, (3) main faults, (4) other faults, (5) fault planes.

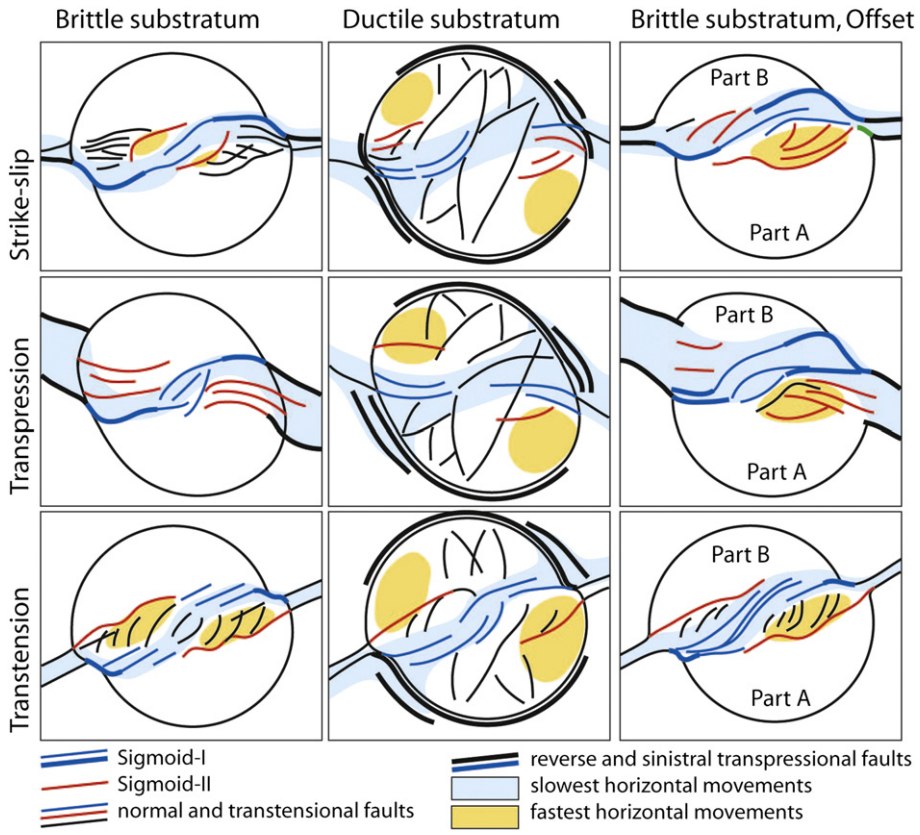

Fig. 8. Main structures developing in cones located in the vicinity of sinistral strike-slip, transpressional and transtensional fault zones.

The bulk of measurements made at the cone summit, including the central part of Sigmoid-I, the other summit grabens and their elongation directions, indicate that the summit systematically undergoes a fast subsidence, especially in strike-slip and transtensional experiments. The strike of the summit graben depends of the regional fault geometry. In brittle experiments, the summit structures develop with an angle of 40° (strike-slip experiments), 60° (transpressional experiments) and 30° (transtensional experiments) from the regional fault zone (Fig. 9). These structures correspond to tension features, similar to strike-slip fault tension structures, which develop with a greater angle to the regional fault zone as its compressional component of movement increases. This important result indicates that the elongation direction of the summit graben can be used to determine the orientation of the stress field around a volcano.

4.3. Ductile substratum experiments

In ductile substratum experiments, the material is transported in a direction that is imposed by the fault movement. The spreading is expressed by radial extension in the cone where the matter is transported from the summit area (extension) toward the cone base (compression). The spreading increases the amplitude of fault movements, especially in the cone lower flank area. The maximum velocity is obtained in the cone lower flanks where the spreading and fault movements have the same direction and are summed.

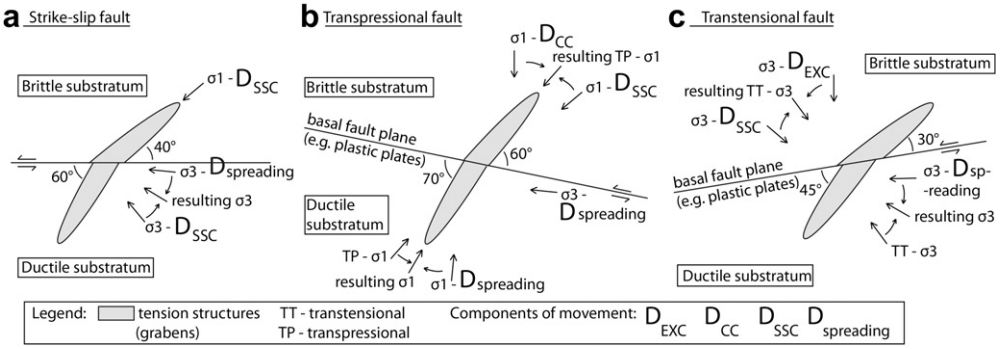

Fig. 9. Orientation of tension features (e.g. grabens located at the cone summit) in sinistral (a) strike-slip, (b) transpressional and (c) transtensional experiments. For brittle substratum experiments, the summit graben develops in the stress field of the D_{SSC} that is rotated by the additional D_{EXC} or D_{CC}. The resulting stress field corresponds to that of transtensional or transpressional faults and is itself rotated by the gravitational spreading movements when a ductile layer is added to the substratum.

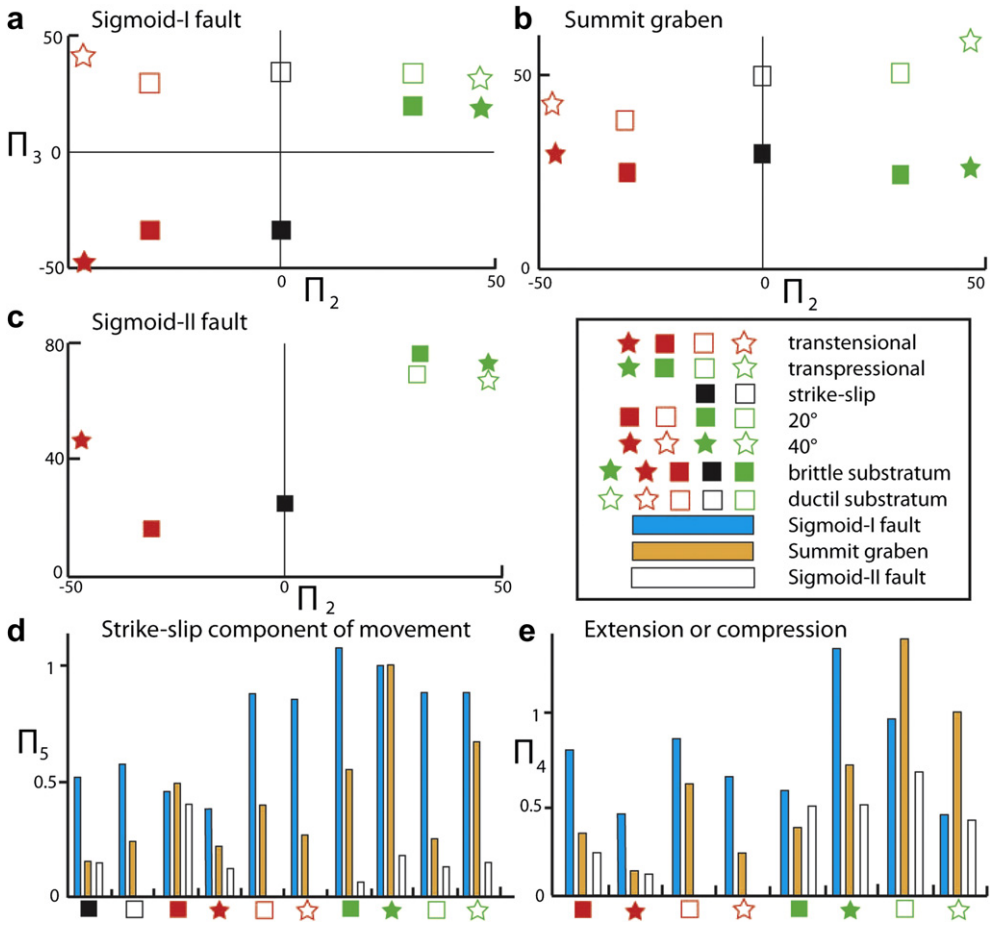

Fig. 10. a-c) Plot of II_2 versus II_3 for Sigmoid-I and II and for the summit graben; II_2 is the percentage of D_{EXC} and D_{CC} over D_{SSC}; II_3 is the percentage of $D_{EXC\text{-}C}$ and $D_{CC\text{-}C}$ for cone faults; the compression ($D_{CC\text{-}C}$, D_{CC}) is negative; d-e) Plot of $D_{EXC\text{-}C}$, $D_{CC\text{-}C}$ and $D_{SSC\text{-}C}$ of cone faults (II_5) showing that most movements are accommodated by Sigmoid-I and, to a lesser extent, by the summit graben.

This confirms, in term of strain, what van Wyk de Vries and Merle (1998) proposed from a simple theoretical stress analysis.

The strike of Sigmoid-I and II faults depends of the regional fault geometry and is unchanged by spreading movements. The spreading increases the extensional component of the faults and may change their kinematics. For example, the Sigmoid-I of strike-slip and transpressional experiments is transpressional above a brittle substratum and is transtensional in ductile substratum experiments. The fault zone is turned into a graben for all fault geometries but large-scale subsidence of this graben is restricted to transtensional experiments. Several long and shallow grabens, which are not observed in brittle substratum experiments, develop at the summit.

Folds and reverse faults develop in the substratum, at the base of the volcano. These structures are better developed at the base of Sigmoid-I, where the spreading and the regional fault movements have opposite directions, and are little expressed at the base of the fastest moving area.

Compared with brittle experiments, the summit structures of cones located above a ductile substratum develop with a greater angle from the regional fault zone: 60° (strike-slip fault), 70° (transpressional fault) and 45° (transtensional fault; Fig. 9). The summit grabens are rotated 10°–20° from the brittle substratum grabens because they tend to be orthogonal to the area of fastest extension (e.g. lower flank area located E and W of the fault zone). The elongation of the summit graben of a spreading cone is thus dependent of the local stress field of the volcanic cone and is not a good indicator of the regional fault-related stress field.

4.4. Offset between cone summit and fault zone

In Offset experiments, the extension along part A faults is greater than in previous experiments and compression dominates along part B faults. Part A-Sigmoid-II and part B-Sigmoid-I delimit the broadest fault zone. These observations lead to the conclusion that the smaller part B flank is extruded. This flank slides along part A-Sigmoid-II fault and toward part B-Sigmoid-I faults. Note that this result shares similarities with those obtained from analogue models of cones and reverse faults interactions (Tibaldi, 2008; Merle et al., 2001; Branquet and van Wyk de Vries, 2001). However, the part B flank is extruded symmetrically by a regional reverse fault while, in Offset experiments, part B flank moves faster where it contains part A-Sigmoid-I and part B-Sigmoid-II and only half of part B flank is extruded.

4.5. Dimensionless analysis

This section focuses on the analysis of dimensionless numbers, which provide data on the kinematics of the faults that develop in the cone (e.g. Sigmoid-I and II, summit graben). The thickness of the fault zone (II_1) is the same for all the cone slopes and sizes tested. The II_1 number increases from strike-slip ($II_1 = 0.2$), transpressional

($\Pi_1 = 0.25$–0.32 for $\alpha = 20°$; $\Pi_1 = 0.28$–0.35 for $\alpha = 40°$) and transtensional experiments ($\Pi_1 = 0.27$ for $\alpha = 20°$; $\Pi_1 = 0.29$–0.41 for $\alpha = 40°$). The addition of a ductile substratum did not significantly modify Π_1.

The analysis of dimensionless numbers indicates that the larger the extensional component of the regional fault (D_{CC} to D_{EXC}, e.g. Π_2), the more Sigmoid-I accommodates extension (Π_3 increases). Sigmoid-I has usually the same kinematics as the regional fault plane, with the exception of the Sigmoid-I developing in strike-slip experiments (Fig. 10-a) and is thus the continuation of the regional fault Y plane (Sylvester, 1988) inside the cone. The fault is always transtensional, and accommodates a similar amount of extension for all Ductile substratum experiments (Fig. 10-a).

Sigmoid-II is not a well developed fault in transpressional and strike-slip experiments for which it accommodates mostly strike-slip movements (large $D_{SSC\text{-}C}$ and small $D_{EXC\text{-}C}$, e.g. Fig. 10-c). The $D_{EXC\text{-}C}$ of Sigmoid-II is larger in transtensional experiments because it borders the graben that develops above the regional fault plane.

In the cone, the strike-slip component of movement is mostly accommodated by Sigmoid-I and, to a lesser extent, by the summit graben (Fig. 10-d). The extensional and compressional components of movement are also mostly accommodated by Sigmoid-I (Fig. 10-e). The transtensional experiments are an exception as the extension is also accommodated by the Sigmoid-II fault (Fig. 10-e). This observation confirms that Sigmoid-I, which accommodates most of the movements, may be regarded as a curved Y shear. Sigmoid-II is a by-product of the uplift which develops in transpressional and strike-slip experiments. This fault only accommodates an important amount of dip-slip movement in transtensional experiments because it borders the graben that develops above the regional fault plane. The addition of a ductile layer did not significantly modify the distribution of movements.

The summit graben, or central part of Sigmoid-I in brittle substratum experiments, accommodates the same amount of extension for all the brittle substratum experiments. The addition of a ductile substratum to the experimental device increases its $D_{EXC\text{-}C}$ relative to $D_{SSC\text{-}C}$ (e.g. Π_3, Fig. 10-b). The slip-rate and sense of motion of this fault are independent of that of the regional fault because this structure is formed by D_{SSC} and is thus similar to the tension structures of strike-slip faults. It is little influenced by the compressional and extensional components of movement, which only modify its strike.

5. Conclusions

Analogue experiments made with deformed cones of granular material have been used to determine the location, kinematics, strike and slip of faults that develop in a cone located above strike-slip, transtensional and transpressional regional faults. The cone responds to the regional fault movement by developing a complex set of faults. One of these faults is named Sigmoid-I. It is synthetic (e.g. same sense of motion) and has the same kinematics (e.g. strike-slip, transtensional or transpressional) as the regional fault with the exception of its central summit graben part and with the exception of strike-slip experiments. This major structure accommodates most of the movements and corresponds to a Y shear structure. The second fault is named Sigmoid-II and accommodates an increasing proportion of the deformation as the extensional component of the regional fault increases, and is thus well developed only for transtensional experiments. The movements inside the cone are organised around an uplifted area (strike-slip and transpressional experiments) or a subsiding area (transtensional experiments). The elongation direction of the summit graben can be used to determine the orientation of the main horizontal contraction, or stress, to which it is parallel. The addition of a ductile substratum modifies the kinematic of Sigmoid-I and forms broad shallow grabens parallel to the main horizontal stress and to the regional fault zone.

In Brittle experiments, the fault zone encloses the fastest horizontal movements and corresponds to the most unstable area of the cone, which comprises the cone's summit and a part of its flanks. In Ductile substratum experiments, the fastest movements are located at the periphery of the fault zone and affect a restricted portion of the lower flanks. When there is an offset between the cone summit and the regional fault, the western part of Sigmoid-I and II is atrophied and their eastern part is well developed, which leads to the extrusion of the NE cone flank (for cones located north of left-lateral fault with and E-W striking D_{SSC}). There is a strong, probable relationship between the fast moving and extruding analogue cone flanks and the natural sector collapses. This relationship is explored in the second part of this article.

Acknowledgment

The authors wish to thanks Dr. D. Andrade for his helpful comments. The PhD of L. Mathieu has been funded by IRCSET (Irish Research Council for Science, Engineering and Technology), which is gratefully acknowledged. The models were run at Laboratoire Magmas et Volcans, Université Blaise-Pascal.

References

Andrade, D., 2009. The Influence of Active Tectonics on the Structural Development and Flank Collapse of Ecuadorean Arc Volcanoes. PhD Thesis, Blaise-Pascal University, Clermont-Ferrand, France, p. 240.

Belousov, A., Walter, T.R., Troll, V.R., 2005. Large-scale failures on domes and stratocones situated on caldera ring faults: sand-box modeling of natural examples from Kamchatka, Russia. Bulletin of Volcanology 67 (5), 457–468.

Borgia, A., 1994. Dynamic Basis of volcanic spreading. Journal of Geophysical Research-Solid Earth 99 (B9), 17791–17804.

Borgia, A., Delaney, P.T., Denlinger, R.P., 2000. Spreading volcanoes. Annual Review of Earth and Planetary Sciences 28, 539–570.

Bourne, S.J., England, P.C., Parsons, B., 1998. The motion of crustal blocks driven by flow of the lower lithosphere and implications for slip rates of continental strike-slip faults. Nature 391 (6668), 655–659.

Branquet, Y., Van Wyk de Vries, B., 2001. Effets de la charge des édifices volcaniques sur la propagation de structures régionales compressives: exemples naturels et modèles expérimentaux. (Effects of volcanic loading on regional compressive structures: new insights from natural examples and analogue modelling). Comptes Rendus de l'Académie des Sciences - Series IIA - Earth and Planetary Science 333 (8), 455–461.

Corpuz, E., Laguerta, E., Alanis, P., Marilla, J., Lendio, M., Gabinete, E. & Bacolcol, T., 2004. Volcanic and Crustal Motions from GPS and Ground Deformation Measurements at Mayon Volcano, Philippines. International Union of Geophysical Sciences, 32nd International Geological Congress, Florence, Italy.

Delcamp, A., van Wyk de Vries, B., James, M.R., 2008. The influence of edifice slope and substrata on volcano spreading. Journal of Volcanology and Geothermal Research 177 (4), 925–943.

Donnadieu, F., Merle, O., 1998. Experiments on the indentation process during cryptodome intrusions: new insights into Mount St. Helens deformation. Geology 26 (1), 79–82.

Dusquenoy, T., Barrier, E., Kasser, M., Aurelio, M., Gaulon, R., Punongbayan, R., Rangin, C., Team, F.-F.C., 1994. Detection of creep along the Philippine fault: first results of geodetic measurements on Leyts Island, central Philippines. Geophysical Research Letters 21, 975–978.

Groppelli, G., Tibaldi, A., 1999. Control of rock rheology on deformation style and slip-rate along the active Pernicana Fault, Mt. Etna, Italy. Tectonophysics 305 (4), 521–537.

Holohan, E., van Wyk de Vries, B., Troll, V., 2008. Analogue models of caldera collapse in strike-slip tectonic regimes. Bulletin of Volcanology 70 (7), 773–796.

Lagmay, A.M.F., van Wyk de Vries, B., Kerle, N., Pyle, D.M., 2000. Volcano instability induced by strike-slip faulting. Bulletin of Volcanology 62 (4), 331–346.

Mathieu, L., 2010. The Impact of Strike-Slip Movements on the Structure of Volcanoes: A Case Study of Guadeloupe, Maderas and Mt Cameroon Volcanoes. Ph.D. Thesis, Trinity College Dublin, Ireland, p. 152.

Mathieu, L., van Wyk de Vries, B., Pilato, M., Troll, V., 2011. The interaction between volcanoes and strike-slip, transtensional and transpressional fault zones: Analogue models and natural examples. J. Struct. Geol., in press, doi:10.1016/j.jsg.2011.03.003.

Merle, O., Borgia, A., 1996. Scaled experiments of volcanic spreading. Journal of Geophysical Research-Solid Earth 101 (B6), 13805–13817.

Merle, O., Vendeville, B., 1995. Experimental modelling of thin-skinned shortening around magmatic intrusions. Bulletin of Volcanology 57 (1), 33–43.
Merle, O., Vidal, N., van Wyk de Vries, B., 2001. Experiments on vertical basement fault reactivation below volcanoes. J. Geophys. Res. 106 (B2), 2153–2162.
Norini, G., Lagmay, A.M.F., 2005. Deformed symmetrical volcanoes. Geology 33 (7), 605–608.
Norini, G., Capra, L., Groppelli, G., Lagmay, A.M.F., 2008. Quaternary sector collapses of Nevado de Toluca volcano (Mexico) governed by regional tectonics and volcanic evolution. Geosphere 4 (5), 854–871.
Sylvester, A.G., 1988. Strike-slip faults. Geological Society of America Bulletin 100 (11), 1666–1703.
ten Grotenhuis, S.M., Piazolo, S., Pakula, T., Passchier, C.W., Bons, P.D., 2002. Are polymers suitable rock analogs? Tectonophysics 350 (1), 35–47.
Tibaldi, A., 2008. Contractional tectonics and magma paths in volcanoes. Journal of Volcanology and Geothermal Research 176 (2), 291–301.
van Bemmelen, R., 1953. Relations entre le volcanisme et la tectogénèse en Indonésie. Bulletin of Volcanology 13 (1), 57–62.
van Wyk de Vries, B., Merle, O., 1998. Extension induced by volcanic loading in regional strike-slip zones. Geology 26 (11), 983–986.
Wooller, L., van Wyk de Vries, B., Cecchi, E., Rymer, H., 2009. Analogue models of the effect of long-term basement fault movement on volcanic edifices. Bulletin of Volcanology 71 (10), 1111–1131.